

Module-Power Prediction from PL Measurements using Deep Learning

Mathis Hoffmann^{1,2}, Johannes Hepp^{2,3}, Bernd Doll^{2,3,4}, Claudia Buerhop-Lutz³, Ian Marius Peters³,
Christoph Brabec^{2,3,4}, Andreas Maier^{1,4}, and Vincent Christlein¹

¹Pattern Recognition Lab, Friedrich-Alexander-Universität Erlangen-Nürnberg, Erlangen, 91058, Germany (FAU)

²Materials for Electronics and Energy Technology, FAU

³Helmholtz Institut Erlangen Nürnberg, Erlangen, 91058, Germany

⁴Graduate School of Advanced Optical Technologies, Erlangen, 91058, Germany

Abstract— The individual causes for power loss of photovoltaic modules are investigated for quite some time. Recently, it has been shown that the power loss of a module is, for example, related to the fraction of inactive areas. While these areas can be easily identified from electroluminescence (EL) images, this is much harder for photoluminescence (PL) images. With this work, we close the gap between power regression from EL and PL images. We apply a deep convolutional neural network to predict the module power from PL images with a mean absolute error (MAE) of $4.4 \pm 4.0\%$ or $11.7 \pm 9.5 \text{ W}_P$. Furthermore, we depict that regression maps computed from the embeddings of the trained network can be used to compute the localized power loss. Finally, we show that these regression maps can be used to identify inactive regions in PL images as well.

Index Terms—photoluminescence, power, regression, deep learning, weakly supervised

I. INTRODUCTION

Recently, photovoltaic (PV) power production has grown significantly as a result of the countermeasures to fight global warming. For example, the worldwide production has grown from 190 TW h in 2014 to 720 TW h in 2019 [1]. This is an increase by 379%. To ensure constant performance of the power plants, regular inspection is required, since modules might be damaged during manufacturing, transport or installation. This raises the need for fast, accurate and non-invasive inspection methods.

In the last years, electroluminescence (EL) has been widely adopted by the community as a useful tool to conduct inspection of solar modules [2], [3], [4], [5], [6]. It allows to identify many types of defects. In particular, disconnected parts of the solar module that do not contribute to the power production (inactive areas), clearly stand out [7]. Previous works have shown that the number of cracks is loosely correlated to the power loss [8] and that the power loss of a module is proportional to the fraction of inactive area, as long as it remains small [9]. Recently, Hoffmann *et al.* [10] used deep learning to determine the module power from EL measurements. They introduce a visualization technique that allows to quantify the power loss of individual defects or cells as predicted by the model.

This project has been supported by IBC Solar AG and the German Federal Ministry for Economic Affairs and Energy (FKZ: 0324286 (iPV4.0) and 032429A (COSIMA)). Furthermore, we acknowledge the PV-Tera grant by the Bavarian State Government (No. 44-6521a/20/5).

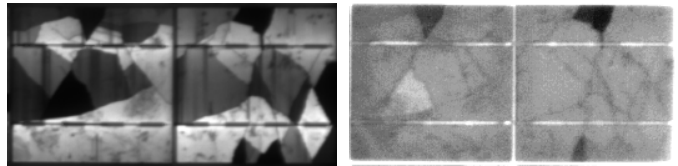


Fig. 1: Comparison between electroluminescence (left) and photoluminescence (right) image of the same module.

However, EL imaging comes at a price, since it requires to disconnect and power the string or module. Only recently, photoluminescence (PL) imaging has become popular on an industrial scale. As opposed to EL, the modules are excited by a light source and no external powering of modules is required. On the downside, inactive areas do not always show as black areas any more (Fig. 1). Instead, they appear with various different intensity levels. This has been previously reported by Doll *et al.* [11].

In this work, we show that the deep learning-based approach [10] can be used to determine the power from PL images of a module, too. To this end, we compile a dataset of 54 module PL images along with measurements of the peak power P_{mpp} and retrain the method using the new data. Furthermore, we investigate, if fine-tuning the models that have been released [10] can improve the performance even further. Finally, we show that the visualization technique using class activation maps (CAMs) can be used to identify the inactive areas on PL images.

II. METHODOLOGY

We aim to estimate the power at the maximum power point P_{mpp} under STC conditions. Here, we use the same approach proposed by Hoffmann *et al.* [10] and estimate P_{mpp} relative to the nominal power P_{nom} . This is a sensible approach, since it assures that the estimates \hat{y} are in a similar scale, independent of the nominal power of a module. Then, we obtain the absolute power as

$$\hat{P}_{\text{mpp}} = \hat{y} \cdot P_{\text{nom}}. \quad (1)$$

In this work, \hat{y} is computed by linear regression from the embedding of a ResNet18 [14]:

$$\hat{y} = \mathbf{W}_{\text{fc}} \mathbf{f}_{\text{emb}}, \quad (2)$$

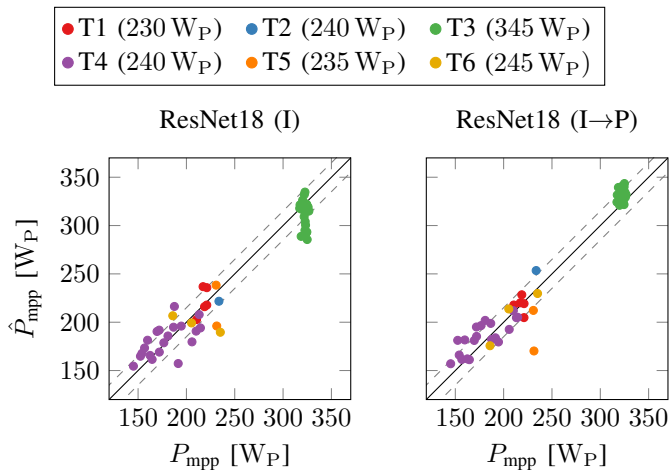


Fig. 2: Distribution of estimation errors comparing pretraining on ImageNet [12] or pretraining on the ELPVPower dataset [13]. We aggregate the results from all three folds of the cross validation. As a result, all 54 samples from the dataset are shown here. The module types are differentiated by color and the respective nominal powers are given by the legend. In addition, the ideal regression line — and the $0 \pm 15 W_P$ iseline - - - are shown.

where $f_{\text{emb}} \in \mathbb{R}^{512}$ is given by $f_{\text{emb}} = f(x, \mathbf{W})$, f represents the ResNet18, \mathbf{W} the parameters of f and \mathbf{W}_{fc} is the linear regression.

We jointly optimize the parameters of the linear regression \mathbf{W}_{fc} and the parameters of the ResNet18 to minimize the mean squared error for all N samples in the training dataset, which is given by

$$L = \frac{1}{N} \sum_{i=1}^N (\hat{y}_i - y_i)^2. \quad (3)$$

As common with deep learning approaches, this is done by batch gradient descent. Except for the weight decay λ , we use the same hyperparameters that have been reported in the prior work. We found that the network seriously overfits to the training data with the reported setting for λ . This is explained by the dataset size, which is much smaller compared to the PVPower dataset [13] used with the reference approach. We heuristically set $\lambda = 0.1$, which consistently gives good results.

Regression maps

Hoffmann *et al.* [10] propose to use a modified variant of CAMs to compute regression maps that give rise to a localized quantification of power losses. In the conventional ResNet18, f_{emb} is computed by averaging over the 512 feature maps. This is commonly referred to as global average pooling. However, by averaging over the spatial dimensions of the feature maps, the spatial information, which is needed for the localized quantification of power losses, is lost. To this end, they propose to apply a 1×1 convolution to the feature maps, reducing the 512 maps to a single one, while preserving the spatial information. Then, they compute the absolute value and multiply the result by -1 . This ensures that the resulting

TABLE I: Results computed by cross validation. The numbers are averaged over all test folds. Furthermore, we show the standard deviation of the MAE.

	MAE		RMSE	
	[%]	[W _P]	[%]	[W _P]
ResNet18 (I)	5.1 ± 4.2	13.9 ± 11.3	6.6	17.9
ResNet18 (I→P)	4.4 ± 4.0	11.7 ± 9.5	5.9	15.1
sample mean	9.6 ± 5.5	26.0 ± 12.3	11.0	28.8

regression map f_{map} is strictly negative. The relative power \hat{y} is then computed as

$$\hat{y} = 1 + \sum_{i,j \in \Omega_f} \underbrace{-\text{ReLU}(f_{i,j})}_{f_{\text{map}}}. \quad (4)$$

This way, the network can be trained using only the relative power of the module as supervision signal, while the localized power loss is obtained in a weakly supervised manner. The power loss per cell is computed by integrating over the corresponding area of f_{map} . This approach has shown promising results on EL images already. In the following, we show that it performs well on PL images as well.

III. EXPERIMENTS

In our experiments, we focus on two aspects. First, we show that the power of a module can be estimated from a PL image of a module despite the fact that inactive areas are not clearly visible from those images in any case. Second, we show that the regression maps can be used to locate disconnected areas on the module.

A. Data

For our experiments, we use a small dataset of only 54 PL images. These images have been recorded under lab conditions with a front-illuminated SI camera with 2048^2 pixels. Photo excitation has been conducted using our LED PL setup, which has been previously reported [11].

The dataset covers 6 different types of modules, which we denote as T1-T6, with nominal powers ranging from $230 W_P$ to $345 W_P$ and maximum powers ranging from $145 W_P$ to $327 W_P$. The modules of type T1-T2 and T4-T6 feature 60 cells arranged in 10 columns, while T3 has 72 cells in 12 columns.

Prior to processing by the network, images are preprocessed. Here, images are cropped and scaled to a common resolution. Furthermore, they are normalized such that the mean intensity μ over all images computes as $\mu = 0$ and the standard deviation σ is $\sigma = 1$. During training, we apply online data augmentation similar to the reference method. This includes random horizontal and vertical flips as well as slight rotations of the images.

B. Results

Since the dataset is small, it is challenging to draw meaningful conclusions from the result. To overcome this issue, we conduct a three-fold cross validation (CV) and join the results

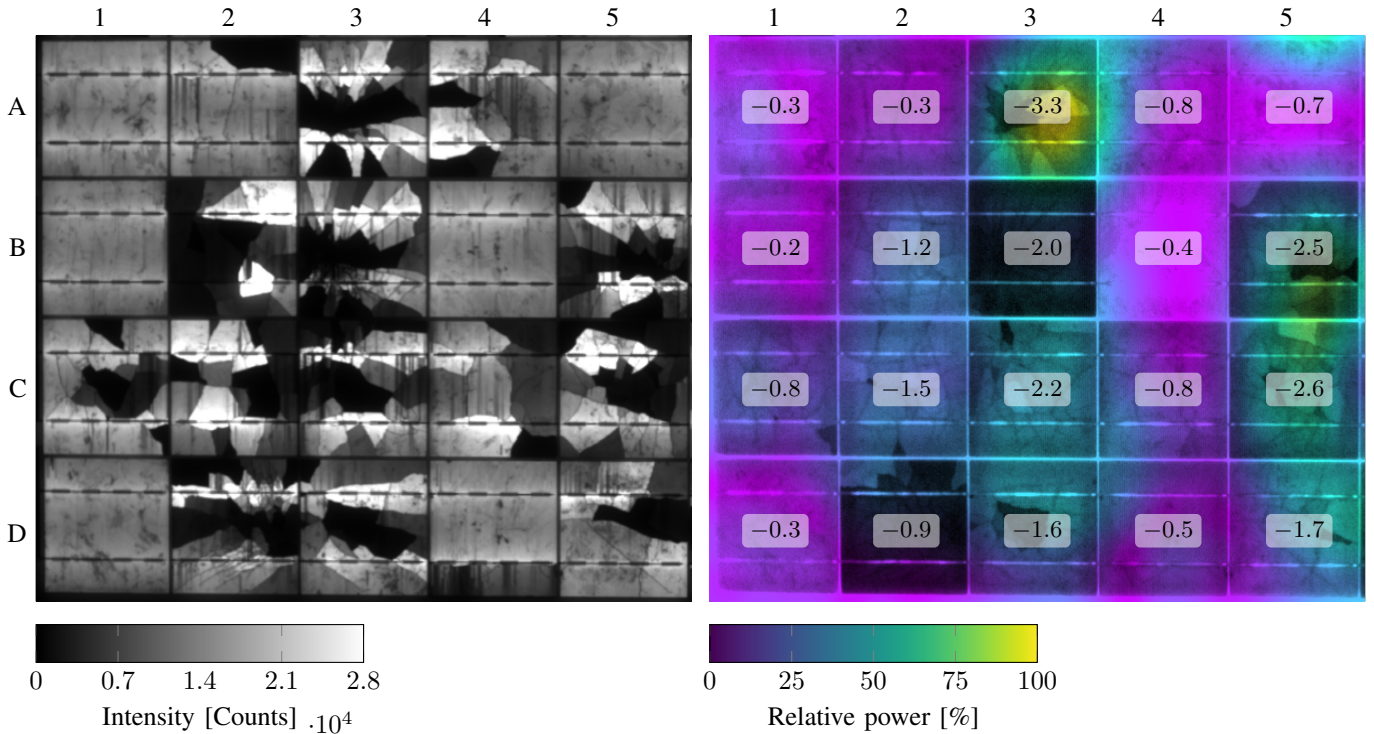


Fig. 3: Quantification of the per-cell power loss using CAMs from a modified ResNet18 (right) in comparison to an acEL image of the same module (left). We color-code the original EL measurement with the given colormap. Note that brighter colors correspond to regions with high relative power loss. Color-coding is done such that the intensity is given by the original image. As a result, color appearance does not exactly correspond to the legend. For every cell, we integrate over the corresponding area of the CAM and multiply the result by P_{nom} . This results in the power loss determined by the model in W_P .

of all folds. Here, we perform a stratified split, such that the distribution of y is similar for all three folds.

We train two different variants of the model. First, we stick to the procedure from the reference method and initialize the network with weights computed by pretraining on ImageNet. We denote this variant ResNet18 (I). Second, we use the weights that has been published with the reference implementation for initialization. Since this has first been trained on ImageNet and then finetuned on the PVPower dataset [13], we denote this variant ResNet18 (I→P). The results are summarized by Tab. I and Fig. 2. Here, we also include a baseline that is computed by calculating the mean of y over every sample of the respective training set and use the result as the prediction \hat{y} for every sample of the corresponding test set. This gives a lower bound to the error. Every model that is better than weighted random predictions should surpass this lower bound. From Tab. I we see that, despite the very small dataset, both variants perform much better than the baseline. Furthermore, we observe that pretraining on the PVPower dataset improves the results slightly.

Finally, we show an exemplary regression map in Fig. 3 and compare it to the EL image of the same module. In summary, we see that the magnitude of predicted power loss per cell is consistent to the amount of inactive area as seen from the EL image, although the inactive area is not always visible in the PL image. For example, cells C1 and C2 have a similar

appearance in the PL image, although C2 is damaged more severely, which can only be seen from the EL image. However, the model prediction is consistent to the EL image, since C2 is predicted to have a higher power loss. Furthermore, we find that the model recognizes that inactive areas might appear as darker or brighter regions. This can be seen from cells B3 and C5. Although B3 is mostly dark in the PL, whereas C5 has only few dark spots, they are predicted to have a similar power loss.

IV. SUMMARY

We experimentally show that PL images of solar modules can be used to determine the power of a module with a MAE of $11.7 \pm 9.5 W_P$, although inactive areas are not well represented by this modality. To this end, we compile a dataset of 54 PL images along with their powers and train a deep neural network to predict the module power. Furthermore, we apply the approach by Hoffmann *et al.* [10] to compute regression maps that allow to quantify the localized power loss. Using these maps, we qualitatively show that the network learns the weakly supervised localization of inactive areas and that the results are consistent to reference EL images.

We are confident that the quantitative results will become better, if a larger training dataset is used. Further, we believe that these preliminary results will amplify research in the field of PL imaging for solar module inspection. For example, they

can help to perform root cause analysis for damaged modules using PL images only.

REFERENCES

- [1] “Solar PV Tracking Report.” <https://www.iaea.org/reports/solar-pv>, 2019. [Online; accessed 18-January-2021].
- [2] M. Köntges, S. Kajari-Schröder, I. Kunze, and U. Jahn, “Crack statistic of crystalline silicon photovoltaic modules,” in *26th EU PVSEC*, vol. 26, pp. 3290–3294, 2011.
- [3] M. Paggi, M. Corrado, and I. Berardone, “A global/local approach for the prediction of the electric response of cracked solar cells in photovoltaic modules under the action of mechanical loads,” *Engineering Fracture Mechanics*, vol. 168, pp. 40–57, 2016.
- [4] M. Mayr, M. Hoffmann, A. Maier, and V. Christlein, “Weakly supervised segmentation of cracks on solar cells using normalized l_p norm,” in *2019 IEEE International Conference on Image Processing (ICIP)*, pp. 1885–1889, IEEE, 2019.
- [5] D. Stromer, A. Vetter, H. C. Oezkan, C. Probst, and A. Maier, “Enhanced crack segmentation (ecs): A reference algorithm for segmenting cracks in multicrystalline silicon solar cells,” *IEEE Journal of Photovoltaics*, 2019.
- [6] S. Deitsch, V. Christlein, S. Berger, C. Buerhop-Lutz, A. Maier, F. Gallwitz, and C. Riess, “Automatic classification of defective photovoltaic module cells in electroluminescence images,” *Solar Energy*, vol. 185, pp. 455–468, 2019.
- [7] C. Buerhop, S. Wirsching, A. Bemm, T. Pickel, P. Hohmann, M. Nieß, C. Vodermayr, A. Huber, B. Glück, J. Mergheim, C. Camus, J. Hauch, and C. Brabec, “Evolution of cell cracks in pv-modules under field and laboratory conditions,” *Progress in Photovoltaics: Research and Applications*, vol. 26, no. 4, pp. 261–272, 2018.
- [8] R. Dubey, S. Chattopadhyay, S. Zachariah, S. Rambabu, K. Hemant, S. A. Kottantharayil, B. M. Arora, K. Narasimhan, N. Shiradkar, and J. Vasi, “On-site electroluminescence study of field-aged pv modules,” in *2018 IEEE 7th World Conference on Photovoltaic Energy Conversion (WCPEC)(A Joint Conference of 45th IEEE PVSC, 28th PVSEC & 34th EU PVSEC)*, pp. 0098–0102, IEEE, 2018.
- [9] E. J. Schneller, R. Frota, A. M. Gabor, J. Lincoln, H. Seigneur, and K. O. Davis, “Electroluminescence based metrics to assess the impact of cracks on photovoltaic module performance,” in *2018 IEEE 7th World Conference on Photovoltaic Energy Conversion (WCPEC)(A Joint Conference of 45th IEEE PVSC, 28th PVSEC & 34th EU PVSEC)*, pp. 0455–0458, IEEE, 2018.
- [10] M. Hoffmann, C. Buerhop-Lutz, L. Reeb, T. Pickel, T. Winkler, B. Doll, T. Würfl, I. M. Peters, C. Brabec, A. Maier, and V. Christlein, “Deep learning-based pipeline for module power prediction from el measurements,” *arXiv preprint arXiv:2009.14712*, 2020.
- [11] B. Doll, H. J., M. Hoffmann, O. Stroyuk, A. Vetter, M. Hemsendorf, D. Tegtmeyer, F. Talkenberg, M. Menz, M. Baier, R. Schüler, L. Lüer, C. Camus, C. Buerhop-Lutz, J. Hauch, I. Peters, and C. Brabec, “Contactless outdoor photoluminescence of silicon photovoltaic modules with large area excitation source,” in *37th EU PVSEC*, pp. 1370–1373, 2020.
- [12] J. Deng, W. Dong, R. Socher, L.-J. Li, K. Li, and L. Fei-Fei, “Imagenet: A large-scale hierarchical image database,” in *2009 IEEE conference on computer vision and pattern recognition*, pp. 248–255, Ieee, 2009.
- [13] C. Buerhop-Lutz and M. Hoffmann, “ELPVPower: A dataset for large scale PV power prediction using EL images,” 2020.
- [14] K. He, X. Zhang, S. Ren, and J. Sun, “Identity mappings in deep residual networks,” in *European conference on computer vision*, pp. 630–645, Springer, 2016.